

May 2013

Sub-sonic Open-return Wind-tunnel and Measurement Apparatus

Michael Adams
Macalester College, michaeladams09@gmail.com

Follow this and additional works at: <https://digitalcommons.macalester.edu/mjpa>



Part of the [Astrophysics and Astronomy Commons](#), and the [Physics Commons](#)

Recommended Citation

Adams, Michael (2013) "Sub-sonic Open-return Wind-tunnel and Measurement Apparatus," *Macalester Journal of Physics and Astronomy*: Vol. 1: Iss. 1, Article 1.

Available at: <https://digitalcommons.macalester.edu/mjpa/vol1/iss1/1>

This Capstone is brought to you for free and open access by the Physics and Astronomy Department at DigitalCommons@Macalester College. It has been accepted for inclusion in Macalester Journal of Physics and Astronomy by an authorized editor of DigitalCommons@Macalester College. For more information, please contact scholarpub@macalester.edu.

Sub-sonic Open-return Wind-tunnel and Measurement Apparatus

Abstract

Wind tunnels are an effective tool for understanding relationships between predicted and actual behavior of air foils in laminar flow. In order to improve the ability of Macalester College staff and students to observe and experiment with the effects of laminar air flow on various objects and systems, it was necessary to construct and test a sub-sonic open return wind tunnel. The purpose of the tests was to discover whether or not the air flow through the test section of the tunnel was laminar around the object being tested and also to evaluate the quality of an apparatus constructed to measure lift and drag within the wind tunnel. I present the results of my tests and analyses as well as comparisons to known data and proven relationships.

Cover Page Footnote

Adviser: Dr. James Doyle Macalester College

Sub-sonic Open-return Wind-tunnel and Measurement Apparatus

Michael Adams

Adviser: Dr. James Doyle

Macalester College

Abstract

Wind tunnels are an effective tool for understanding relationships between predicted and actual behavior of air foils in laminar flow. In order to improve the ability of Macalester College staff and students to observe and experiment with the effects of laminar air flow on various objects and systems, it was necessary to construct and test a sub-sonic open return wind tunnel. The purpose of the tests was to discover whether or not the air flow through the test section of the tunnel was laminar around the object being tested and also to evaluate the quality of an apparatus constructed to measure lift and drag within the wind tunnel. I present the results of my tests and analyses as well as comparisons to known data and proven relationships.

I. Introduction

The concept of a wind tunnel was first proposed by Leonardo Da Vinci in the 16th Century. He is quoted as stating in his work,

“...the action of the medium upon the body is the same whether the body moves in a quiescent medium, or whether the particles of the medium impinge with the same velocity upon the quiescent body (Anderson 2008).”

Although this thought did not lead to any immediate practical applications, it was the first recorded example of human understanding of how fluid flow across objects works. The first true wind tunnel was constructed in Greenwich, England by Francis Wenham. This wind tunnel was a very primitive box design and used a steam powered engine to push air through a tunnel and then measured the lift and drag forces using weighing beams attached to the object being tested.

In 1884 the second wind tunnel was built by Horatio F. Phillips. This second tunnel maintained a similar box design to Wenham's, but instead of forcing air through the tunnel he used steam injectors to pull air through. Although this development led to more accurate results, it wasn't until 1901 that truly useful results were obtained in wind tunnels through the efforts of the Wright Brothers.

In 1901 the Wright Brothers worked towards developing the first aircraft. During many of their struggles to create an effective vehicle, they came to the conclusion that most of the data relating to airfoils was incorrect. The data was accepted as right based off of the tests of other experimentalists, but it had no practical application to flight testing and needed to be reevaluated. In response, they created their own 6 foot long and 16 inch squared wind tunnel that was driven by a two blade gas powered engine. In addition to this tunnel they also developed an apparatus

which measured the ratio of lift to drag. Over the course of the next year and half they tested 200 different wing designs and finally found one they thought would be optimum. These results lead to the first flyable aircraft and was also the beginning of the use of modeling to assess the performance of structures before building the full design (Anderson 2008).

Due to the achievements of the Wright Brothers, one of the most important aspects of contemporary engineering is the ability to model and understand how something will work/perform before constructing it. Wind tunnels have been a major advancement in the last century that allowed engineers and designers to see how different constructs behave in varied wind conditions and what relationships there are between different components of design and performance.

In this project, I used many experimentally proven pieces of data to construct a sub-sonic open-return wind tunnel. Once I completed construction of the wind tunnel and built an apparatus to measure the lift and drag of an object in the tunnel, I began running tests on a ball and a flat plate that had an adjustable angle of attack. The purpose of these tests was to determine whether or not this wind tunnel was creating laminar flow within the test section, observe whether or not results could be replicated for known experiments to verify that the tunnel was useful, and to test whether or not the apparatus was useful in making the proper measurements of lift and drag.

II. Methodology

II.1 Wind Tunnel Construction

The most important component of building a wind tunnel is determining which type of wind tunnel is the most practical for your needs and your available resources. After a review of

multiple descriptions the open-return sub-sonic wind tunnel, Figure 1, was determined to be the most practical and simple apparatus to create.

Once this particular tunnel design was selected it was necessary to know what principles governed its operation. The first and most critical component was the assumption that airflow in the tunnel was incompressible. This means that if a small parcel of air was selected and monitored throughout the entire wind tunnel, the density would change negligibly.

Incompressible flow has numerous impacts on the operation of the tunnel. It primarily affects the equations that govern how the velocity in the different sections is related, but it can also have a major impact in the test section if the air is compressing around the air foil being tested. Since interpretations of experiments strongly depend on the type of fluid flow within the tunnel, it is very important to justify the reason for assuming incompressible flow. Since it takes a large amount of force to compress and increase the density of a fluid, a compressible flow would require a high volume of air to be forced into a smaller section very rapidly. To simplify this matter, the velocity in the tunnel would need to exceed the velocity of the individual particles movement within a given volume of air. Through testing it has been observed that this effect does not occur for air velocities under 134.112 m/s (Anderson 2007). Since our tunnel design does not use a powerful enough fan to achieve this velocity or even velocities greater than 10% of this value (max at 9.05 m/s), it is safe to assume that any effects due to compressibility are negligible. With this assumption it becomes possible to use Bernoulli's equation (1) to show how full sized wind tunnels are operated, and through the continuity equation (2) we were able to show the relationship between the velocities in the three main sections of the wind tunnel shown in Figure 1.

$$p_1 + \frac{1}{2} * \rho * V_1^2 = p_2 + \frac{1}{2} * \rho * V_2^2 = p_3 + \frac{1}{2} * \rho * V_3^2 \quad (1)$$

$$\rho * V_1 * A_1 = \rho * V_2 * A_2 = \rho * V_3 * A_3 \quad (2)$$

In these equations ρ (kilogram per meter cubed) is the density of the air, p_1 (Pascals), A_1 (meters squared), and V_1 (meters cubed) are the pressure, cross-sectional area, and volume of the contraction cone, p_2 , A_2 , and V_2 are the pressure, cross-sectional area, and volume of the test section, and p_3 , A_3 , and V_3 are the pressure, cross-sectional area, and volume of the diffuser (Hughes and Brighton 1999).

Once relationships between the sections of the wind tunnel were understood it was important to know what the purpose of each section was and develop a way to make them as effective as possible in producing uniform laminar flow; non-turbulent streamline flow in parallel layers. The open-return tunnel uses a large intake with some sort of collimator in order to draw in air at a low pressure that is laminar in flow. This first section is known as the settling chamber, shown in Figure 3. In the case of this particular wind tunnel design, the settling chamber consists of a honeycomb of 1/8" polycarbonate straws and two wire mesh screens. The purpose of the honeycomb is to produce flow of air parallel to the axis of the tunnel. For this reason, the honeycomb is placed the furthest upstream of the test section at the beginning of the settling chamber. The purpose of the two screens is to make the velocity of the air in the tunnel cross-sectionally consistent. As air flows across the screen, it creates a drop in pressure, which makes the air speed consistent. The first of the two screens was placed 5" from the honeycomb in order to allow the flow of air to settle and reduce turbulence. The second screen was then placed 5" from the first to allow the same reduction in any turbulent effects from the first screen.

The next component of the open-return tunnel is the contraction cone as shown in Figure 4. The purpose of the contraction cone is to increase the velocity of the air as it flows into the test

section by providing a gradual contraction so that no major turbulent effects are created immediately before the test section. The ratio for the inlet to the outlet of the contraction cone is roughly 9:1. This ratio is meant to optimize the area of the contraction cone while avoiding flow separation; condition where turbulent flow along the boundary layer is no longer isolated to the boundary layer and creates turbulence in the main flow of air in the form of eddies and vortices. If the contraction is too large or happens too rapidly, flow separation becomes very common and difficult to avoid. In this case, the inlet to the contraction cone is 3' by 3' and the outlet leading into the test section is 1' by 1' (NASA 2013). Since the inlet and outlet are different sizes it was important to add adjustable legs to the outlet side of the contraction. This allows the section to be adjusted so that it is level with other sections and so that it can rest flat on any surface.

The next section is the test section as shown in Figure 5. The test section is where the object being experimented on is placed and where the flow of air should be completely laminar. The test section needs to be completely smooth so that unnecessary turbulence is not created. This test section was created using 1/8" and 1/4" Plexiglas. The dimensions of the interior were 1' by 1' by 2'. In order to easily modify what is being tested and change objects it is necessary to have access to the interior of the test section. Thus, the top and bottom panels had ports drilled in them that were covered using 1/4" Plexiglas.

The final section is the diffuser as shown in Figure 6. The diffuser is a section that increases in size from its inlet to outlet. The reason for this is to allow an increase in volume and reduction in velocity as air exits the system. This helps prevent any back turbulent effects that may result in problems within the test section. In order to keep flow separation from occurring in this section it is necessary to keep the increase in size very gradual, with an angle of increase between 5-10 degrees (NASA 2013). At the outlet of this section the fan is attached.

The fan is the final component of the wind tunnel. It is set up in such a way that it pulls air through the wind tunnel. This set-up has multiple benefits. First, pulling air through reduces turbulence in comparison to pushing it through. When you pull air you create a down pressure inside the wind tunnel which forces air from further inside the wind tunnel to rush and replace it. This method of using reduced pressure causes a more uniform flow of air since all of the air in the tunnel is subject to the effect of the flowing air almost immediately. On the other hand, when air is pushed through a tunnel, rotational effects are automatically generated in the air flow. It is possible to counter this effect by using flow straighteners, like in the settling chamber mentioned earlier, but in order to maintain the necessary contraction in the tunnel it is necessary to employ a much larger fan. Another major issue with pushing air is that any fluctuation in the tunnel will cause large turbulent effects. If a swirl of air begins in the tunnel, it will have large consequences in the surrounding air flow immediately. These effects are called vortices and they render wind tunnels almost completely ineffective due to the breakdown of laminar flow, much like in the case of flow separation (Anderson 2008). The fan used in this experiment was attached to a Variac with a range of 0-28 volts which produced variable air speeds and thus allowed for a greater possible range of experiments.

11.2 Measurement Apparatus Construction

In order to make a wind tunnel useful, it is necessary to have a device for measurements of the force on the object being tested. For our apparatus the goal was to measure the lift and drag of the object inside the tunnel. Lift is the perpendicular force to air flow acting upon a body within a fluid flow and drag is the component of force that resists motion in the direction of air flow across the test object. This requires independent force measurement for two degrees of freedom but most scales and force sensors only allow for one degree of freedom. By using two Vernier

Dual Range Force Sensors (5N-50N) and creating a special mount, Figure 7, an apparatus was created that took advantage of the freedom of the sensors to move within their cases. This design theoretically allowed us to measure the two desired forces from within the wind tunnel by attaching the object being tested to a post and then running that post through a hole in the bottom porthole of the test section into the measurement apparatus.

11.3 Testing

In order to determine the effectiveness of the wind tunnel and apparatus it was necessary to run multiple tests. The first issue was to resolve how to determine the speed of air flow within the test section. This was accomplished by attaching an anemometer at the outlet of the test section. By varying the voltage from the Variac and then recording the resulting speed within the tunnel over multiple measurements, a calibration curve (see Figure 12) was made so that wind speeds could be set during the experiment without having the anemometer present in the test section. It was necessary to remove the anemometer during experiments because it would create interference in the test section that could compromise the test results.

The next issue to resolve was whether or not the wind speed was consistent at different points within the wind tunnel. Using the same anemometer, the mount was moved to different positions to ensure that the air flow in the test area was consistent. In addition to this, it is necessary to know at what point turbulence along the boundary layer of the wind tunnel wall begins to affect air flow in the test section. By knowing roughly where this occurs it provides insight into what size objects can be used for best test results.

Once it was established that the flow in the test section was uniform, lift and drag tests began. Two objects were used to assess the laminar flow within the tunnel. The first was a sphere

mounted on a post that was attached to the force measurement apparatus to see if there was any lift on it for various wind speeds. The results were recorded by connecting the force sensors to a computer and using the program Logger Pro to collect data over 0.2 second intervals for ten seconds at each speed. For our second experiment, a special mount was constructed for a metal plate that allowed for a variable angle of attack; angle between surface area of plate and flow of air as shown in Figure 13. By running data collection at multiple speeds for many different angles, data was collected for both the lift and drag. Once the known value of lift was recorded it was possible to find the coefficient of lift by using the equation

$$c_l = \frac{L}{\frac{1}{2} \rho v^2 S} \quad (3)$$

where L (Newton's) is the recorded lift force, v (meters per second) is the velocity of air in the wind tunnel, S (meters squared) is the area of the plate, and ρ (kilogram per meter cubed) is the fluid density of air. By calculating the coefficient of lift at the same wind speeds for various angles, relationships could be generated and compared to known results for air foils in wind tunnels and thereby determine whether or not the wind tunnel was effective enough to be used for further research (Anderson 2007).

III. Results and Discussion

III.1 Laminar Flow and Air Speed Consistency

It was observed that at any given point there were wind speed fluctuations of about 0.17 m/s on average. This fluctuation is small when comparing wind speeds from 2.25 m/s to 9.1 m/s, with a highest error of lower than 8% at the lowest wind speeds. When comparing wind speeds for different points within the tunnel the change was small, with a maximum variation of 0.23 m/s.

This variation was deduced to be quite minor when taking into account the stationary fluctuation of wind speeds. Since 0.17 m/s of that variation can be associated with the variation of wind speed between trials, only 0.06 m/s was attributed to the change due to positioning within the test section. Because the objects being tested do not take up large areas orthogonal to the direction of air flow, the variation in wind speed throughout the test section was less than 10% and is small compared to other uncertainties.

III.2 Lift on a Sphere

The next important piece of data came from the testing of lift the effects of airflow on the sphere. Due to the symmetric shape of a sphere, as air passes around it, if the air in the tunnel was truly laminar, then the air would pass across the surface at the same rate and not cause any lift force. 10 different wind speeds were tested and all of the results showed zero lift within the measured uncertainty with force measurements at around 0.002 N; except for the result at 9.05 m/s where a force of -0.01212 N was recorded. For this last result we speculate that either the apparatus has some error that allowed for a small range of fluctuations not attributable to the lift force, the ball was not perfectly round, or the small variations in air speed due to displacement in the wind tunnel had a larger impact than originally thought. By observing the fluctuations in the measurement apparatus it was determined that the first of the possibilities was the correct answer. There were variations recorded on average of roughly 0.01 N even for objects at low wind speeds, so we conclude that there was no lift generated to within the random fluctuation error of the measurement.

III.3 Flat Plate

A more rigorous test of the wind tunnel was the lift and drag on a flat plate at various angles of attack. The only theory for lift on a flat plate comes from using the sine of the angle of attack. This model predicts that the lift should increase linearly as the angle of attack increases, but experimental data and literature (Figure 11) show otherwise. By comparing our results to literature it became necessary to see if this wind tunnel was able to produce relationships that it is supposed to. Figure 8, 9, and 10 show the coefficient of lift versus angle attack for various wind speeds as measured in the wind tunnel. These plots all have lines connecting the points and it is necessary to note that these lines are not representative of a fit, they are only meant to make the overall relationship between the data points more apparent. As can be observed in Figure 8, the relationship between c_l and angle of attack is not very well defined. As the angle of attack and the wind speed becomes larger the trend becomes more like the expected trend given in Figure 11. The best results gathered from the tunnel came at the high wind speeds. Figure 10 is a plot of only the high wind speeds that show the very consistent trend and the similarities to the data in Figure 11. Both our results and the literature show that as the angle of attack reaches 15-18 degrees, c_l begins to decrease and then no more data points are given. The accepted reason for the decrease is that around 15-18 degrees the transition for laminar into turbulent flow occurs closer to the leading edge of the air foil. This means that there is a large amount of turbulent flow on the back side of the air foil. This effect leads to the phenomenon of aircraft stall. Once this critical angle is reached the air foil is no longer able to produce lift that counters the effects of drag and turbulence. The results found in this particular wind tunnel match this trend up to 20 degrees, however, for larger values it was found that the lift starts to increase again for wind speeds above 4 m/s. Because this causes a major problem with the model it was necessary to investigate possible causes of this strange occurrence. While observing the measurement

apparatus at high angles and high wind speeds it was noticed that the rod attaching the airfoil to the measurement device was beginning to flex. In addition to this, there was a torque observed around the point where the drag force is measured which could potentially cause additional “lift force”. Due to these errors in the measurement device it was necessary to conclude that the relationships were still good. An additional reason for assuming that this data can be neglected is because none of the data collected from larger wind tunnels (Figure 11) includes angles above 22 degrees. This made it apparent that this may not be an isolated incident and that there could be a technical reason for ceasing to take data at even higher angles of attack. Since there was no literature to expand upon this issue or detail why these plots did not include further angles, the issue had to be left for future study.

IV. Summary and Conclusion

Based on the results of the tests, this wind tunnel proved to be effective. It produced results that agree with accepted trends and this established confidence that this tunnel can be used in future aerodynamic experiments.

The construction of a sub-sonic open return wind tunnel is a very practical process; however, more time should be put into planning the best way to design different components of the tunnel, especially in regards to the contraction cone. The design could lead to higher increases in velocity in the test section, meaning a smaller fan can be used or less energy to achieve quality wind speeds and more laminar flow. The primary feature that could change this is using a fan that is large enough to give a 3:2 ratio for the outlet to inlet area of the diffuser (NASA 2013). This will help with the increase in velocity through the relationships in equation 2

and will add even higher speeds due to increased power potential in the fan. Another method would be to use two counter-rotating fans.

Future research with this wind tunnel should include the development of a more sensitive measurement apparatus. If highly accurate results are desired and a sufficient budget is available, it would be beneficial to purchase a Multi-Axis Force/Torque Sensor. This device would offer the ability to measure all six components of force and torque. Having this capability would offer a much more comprehensive approach to gauging the effectiveness of this wind tunnel and would also offer opportunities for more significant experiments.

References

1. Anderson, John David. *Fundamentals of Aerodynamics*. Boston: McGraw-Hill Higher Education, 2007. Print.
2. Anderson, John David. *Introduction to Flight*. Boston: McGraw-Hill, 2008. Print.
3. Hanley, Patrick. *Hanley Innovations*. N.p., n.d. Web. Apr. 2013.
<<http://hanleyinnovations.blogspot.com/2012/02/top-10-reasons-to-analyze-your-airfoil.html>>.
4. Hughes, William F., and John A. Brighton. *Schaum's Outline of Theory and Problems of Fluid Dynamics*. New York: McGraw Hill, 1999. Print.
5. "The Web's Where You Study In!" *Wind Tunnel Testing*. N.p., n.d. Web. Sept. 2012.
<<http://www.ustudy.in/node/4072>>.
6. "TunnelSim Open Return 1.0g Beta." *TunnelSim Open Return 1.0g Beta*. N.p., n.d. Web. 10 Apr. 2013.
<<https://www.grc.nasa.gov/WWW/k-12/airplane/tunopen.html>>.

Figure Captions

Figure 1. The general schematic of an open-return wind tunnel

Figure 2. Image of the constructed open-return wind tunnel

Figure 3. Image of the settling chamber (left) leading into the contraction cone (right)

Figure 4. Image of the contraction cone (left) leading into the test section (right)

Figure 5. Image of the test section (middle) leading into the diffuser (right)

Figure 6. Image of the diffuser

Figure 7. Image of the measurement apparatus

Figure 8. Coefficient of Lift versus Angle of attack for velocities between 2.225 and 5.455 m/s

Figure 9. Coefficient of Lift versus Angle of attack for velocities between 5.76 and 7.51 m/s

Figure 10. Coefficient of Lift versus Angle of attack for velocities between 7.51 and 9.095 m/s

Figure 11. NASA results of Coefficient of Lift versus Angle of attack for 3 different airfoils

Figure 12. Table of wind speeds for each voltage

Figure 13. Diagram showing the lift force, drag force, and angle of attack based off of a relative wind

Figures

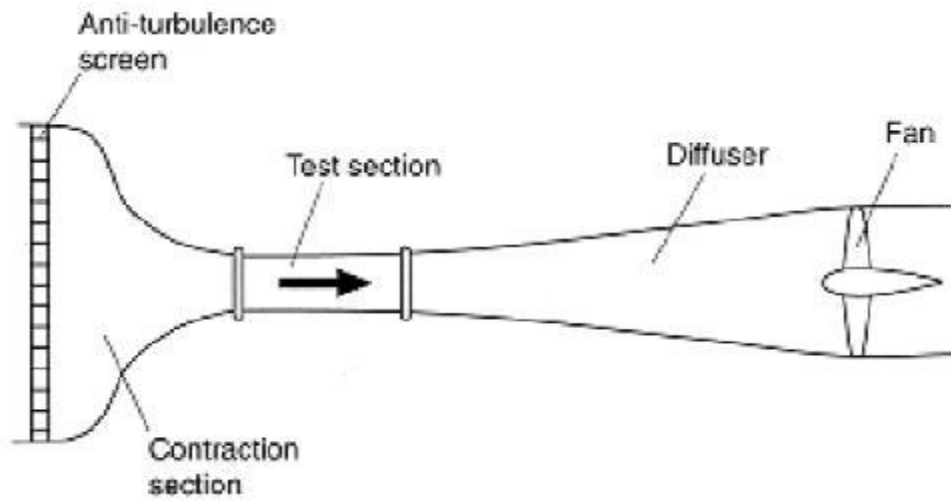


Figure 1



Figure 2



Figure 3

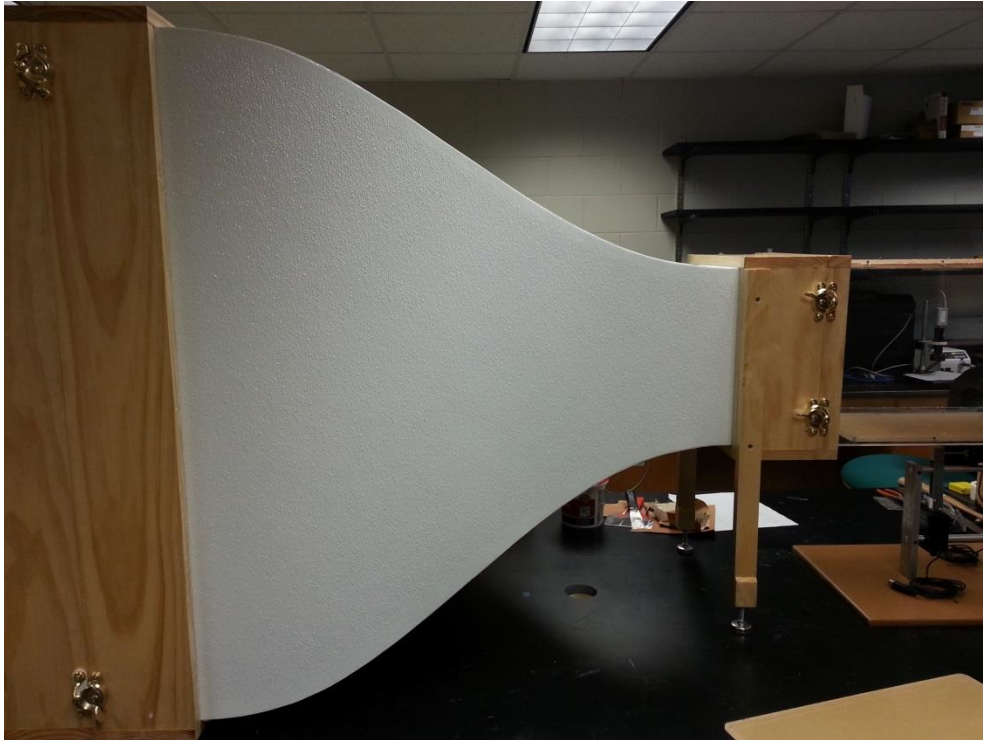


Figure 4



Figure 5



Figure 6

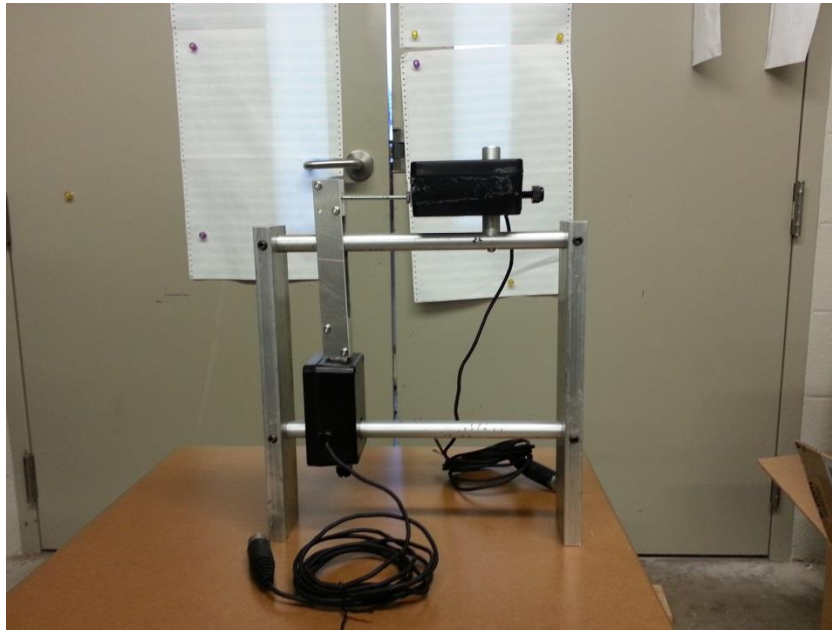


Figure 7

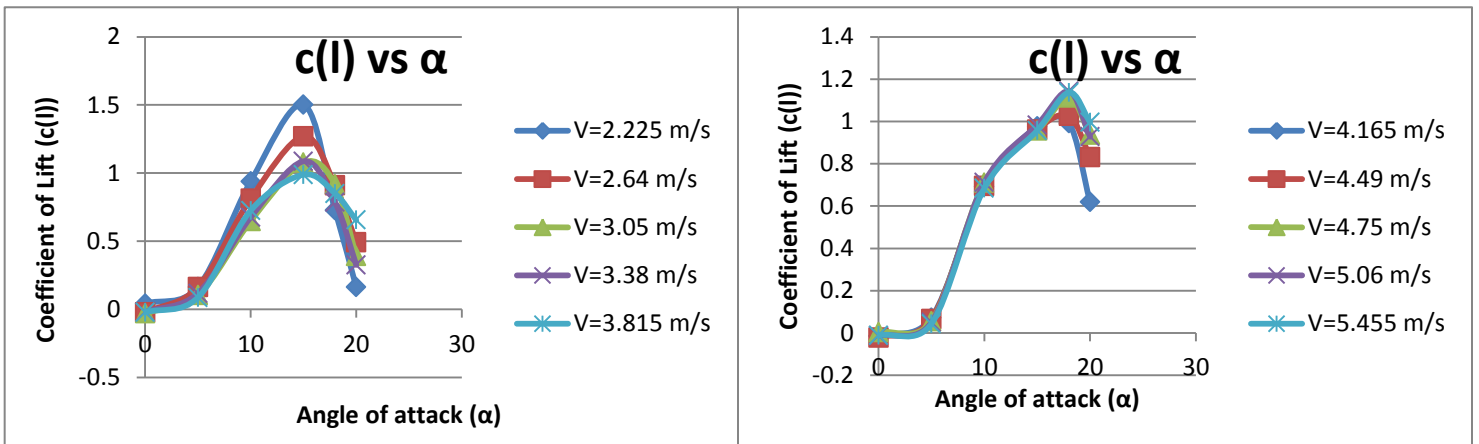


Figure 8

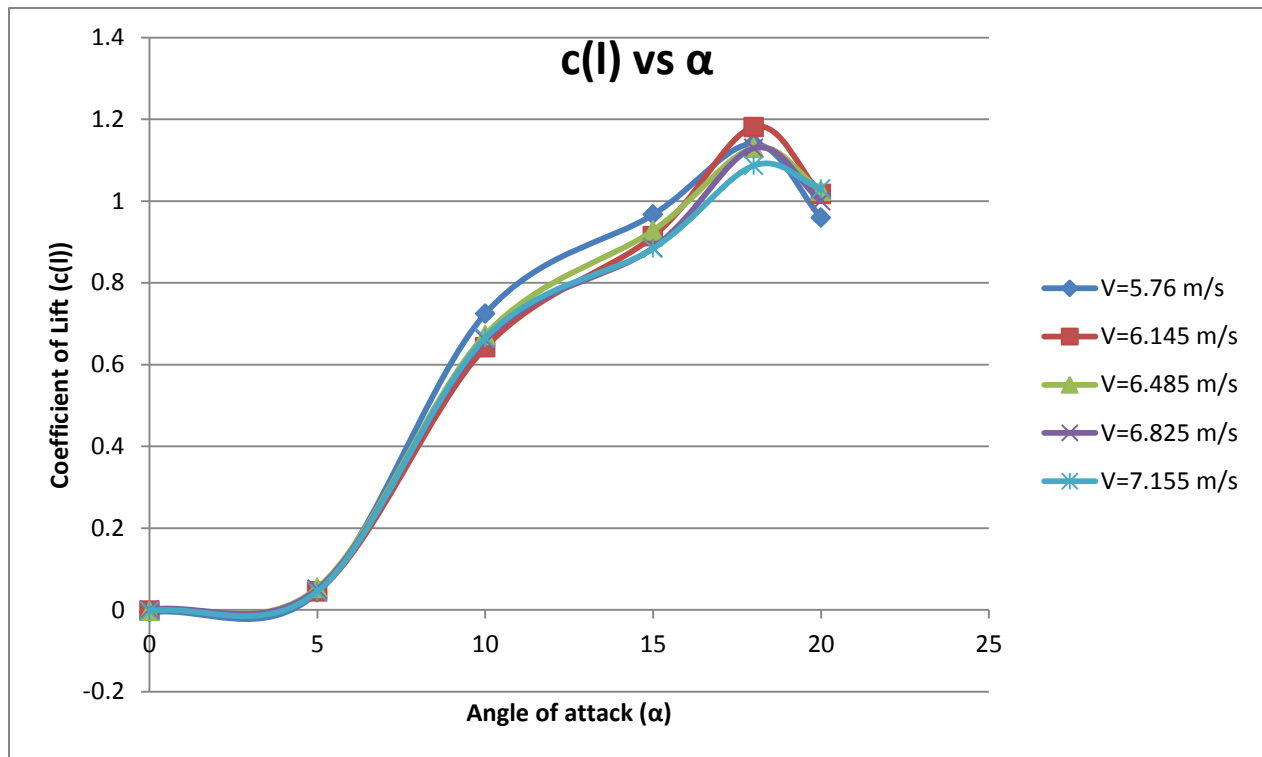


Figure 9

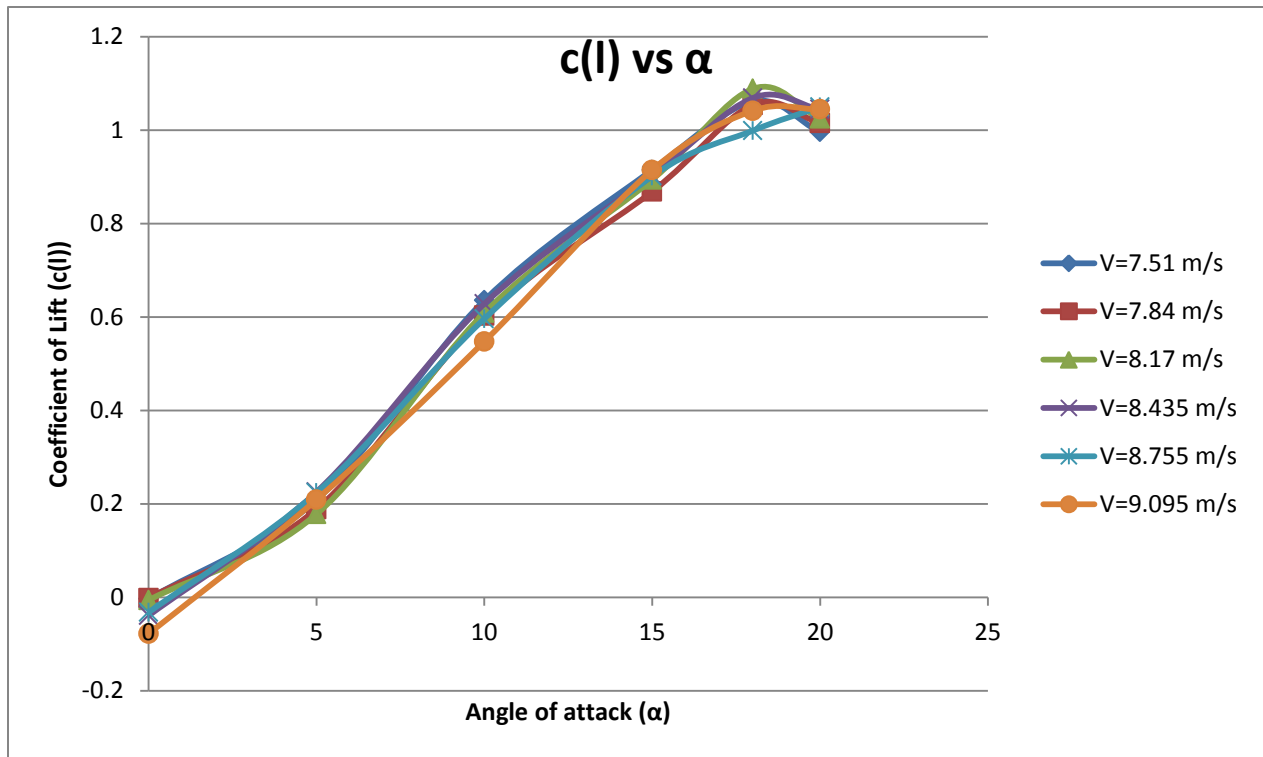


Figure 10

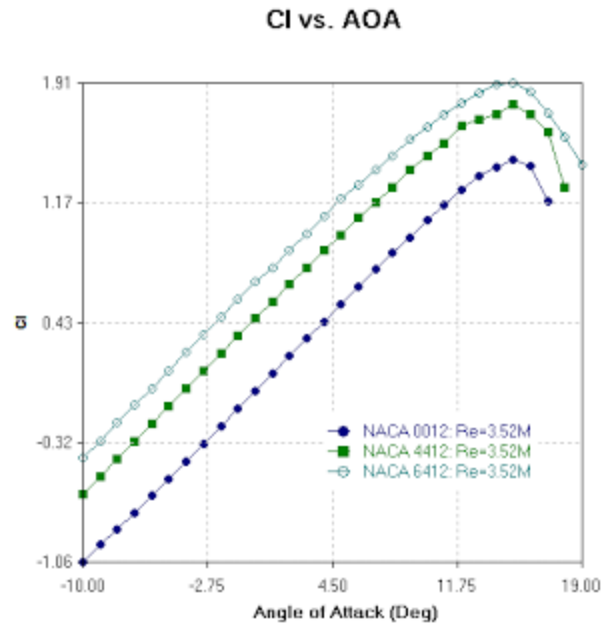


Figure 11

Voltage	3.99	4.52	5.06	5.51	6.07	6.52	7.03	7.55	8.03	8.55	9.05
Velocity (m/s)	2.225	2.64	3.05	3.38	3.815	4.165	4.49	4.75	5.06	5.445	5.76
Voltage	9.54	10.02	10.52	11.03	11.56	12.05	12.58	13.08	13.54	14.08	
Velocity (m/s)	6.145	6.485	6.825	7.155	7.51	7.84	8.17	8.435	8.755	9.095	

Figure 12

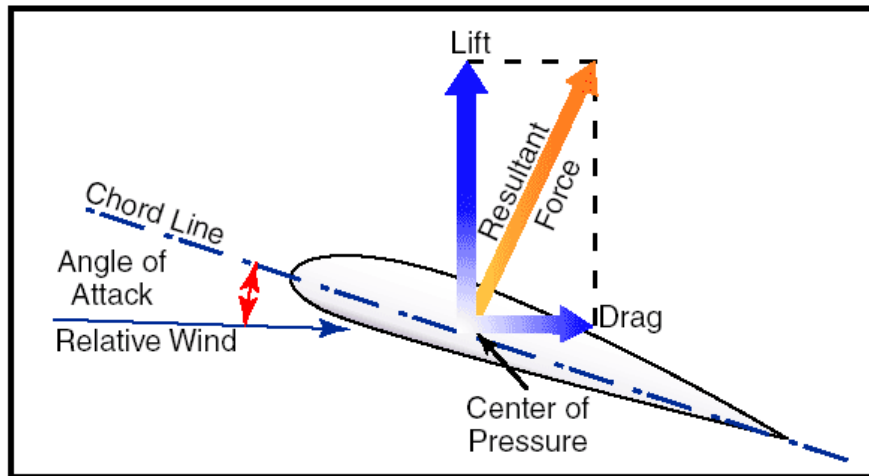


Figure 13